Correlation transfer in stochastically driven neural oscillators over long and short time scales

Aushra Abouzeid and Bard Ermentrout
University of Pittsburgh, Pittsburgh, Pennsylvania, USA
(Received 3 February 2011; published 20 December 2011)

In the absence of synaptic coupling, two or more neural oscillators may become synchronized by virtue of the statistical correlations in their noisy input streams. Recent work has shown that the degree of correlation transfer from input currents to output spikes depends not only on intrinsic oscillator dynamics, but also on the length of the observation window over which the correlation is calculated. In this paper we use stochastic phase reduction and regular perturbations to derive the correlation of the total phase elapsed over long time scales, a quantity that provides a convenient proxy for the spike count correlation. Over short time scales, we derive the spike count correlation directly using straightforward probabilistic reasoning applied to the density of the phase difference. Our approximations show that output correlation scales with the autocorrelation of the phase resetting curve over long time scales. We also find a concise expression for the influence of the shape of the phase resetting curve on the initial slope of the output correlation over short time scales. These analytic results together with numerical simulations provide new intuitions for the recent counterintuitive finding that type I oscillators transfer correlations more faithfully than do type II over long time scales, while the reverse holds true for the better understood case of short time scales.

DOI: 10.1103/PhysRevE.84.061914 PACS number(s): 87.19.lc, 05.45.Xt, 05.40.−a

I. INTRODUCTION

While the jury is still out on the functional role of synchrony and correlations in neural firing, the ubiquity of these phenomena in the nervous system is suggestive. One long-standing hypothesis holds that correlated activity in the visual system underlies feature binding. Synchronous oscillations may also play a role in amplifying signals [1] or transmitting information from one layer to another [2–4], or such oscillations may encode information directly [5–12]. Correlations can be tuned to optimize coherence resonance [13]; on the other hand, correlations may negatively impact the signal-to-noise ratio [14–17], and excessive synchrony is a hallmark of neurological disorders such as epilepsy and Parkinson's disease.

To understand the function of oscillatory correlations, or one day achieve clinically relevant control over them, we must first understand the underlying biophysical mechanisms. While synchrony can arise as the result of anatomical connectivity between neurons, much recent work [18–24] has brought to light ways in which correlated activity develops from the inherent stochasticity of neural systems. Thus, in the absence of direct coupling, two or more neural oscillators may become synchronized by virtue of the statistical correlations in their noisy input streams—a phenomenon we will refer to as stochastic synchrony.

For our analysis of stochastic synchrony, we appeal to the theory of weak coupling, which applies in the stochastic context provided the amplitude of the noise is sufficiently small. In particular, a number of groups [20–22,25] have proved that the phase reduction technique [26] can be applied to oscillators receiving additive noise. Thus, we reduce a noisily driven oscillator to a scalar differential equation describing the evolution of the phase. This so-called phase equation depends only on the properties of the noise and the oscillator's phase resetting curve (PRC), which characterizes how small perturbations influence the oscillator's subsequent timing or phase.

Neural oscillators can be classified into two types according to the bifurcations that occur as the dynamical system goes from a stable rest state to a stable limit cycle. Furthermore, the oscillator's bifurcation class has been shown to determine the shape of its PRC and therefore its ability to synchronize. Type I oscillators undergo the saddle node on an invariant circle bifurcation, and the resulting PRC is strictly positive, indicating that perturbations can only advance the oscillator's phase. Type II cells undergo the Andronov-Hopf bifurcation, which produces a PRC with both negative and positive regions; typically, inputs occurring early in the cycle can delay the phase whereas later inputs advance it. See Fig. 1.

An expanding body of work has demonstrated that over short time scales of less than one period, type II oscillators are more susceptible to stochastic synchrony than type I. This has been shown via simulations and *in vitro* [19,27], by deriving the probability distribution of the phase difference [28], by minimizing the Lyapunov exponent of the phase difference [29], and most recently by calculating the spike count correlation over a range of time windows [30]. The latter study further reports that this finding reverses over long time scales, namely, that type I oscillators transmit correlations more faithfully than type II when observed over lengths of time much greater than one period.

In Sec. II we provide a brief introduction to the phase reduction technique in a stochastic setting. Next, in Sec. III we use regular perturbations to give a novel and straightforward analysis of correlation transfer over long time scales. To facilitate our derivation, we use the total elapsed phase as a proxy for the spike count. Note that the total phase (modulo the period) and the spike count differ by at most one, which is a negligible quantity when many spikes have been observed over a long time window. The expression we derive for the correlation coefficient of the total phase agrees both qualitatively and quantitatively with the results found in Ref. [30].

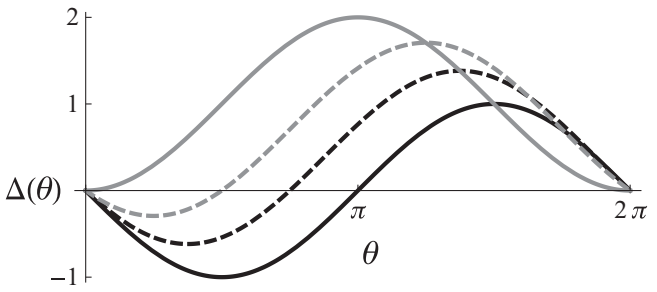

FIG. 1. We use the parametrization $\Delta(\theta) = -\sin(\theta+\alpha) + \sin(\alpha)$ to vary the PRC smoothly from type I (solid gray), where $\alpha = \frac{\pi}{2}$ and $\Delta(\theta) = 1-\cos(\theta)$, to type II (solid black), where $\alpha = 0$ and $\Delta(\theta) = -\sin(\theta)$. Note that intermediate values of α produce PRC shapes (dashed) that more closely resemble those found empirically *in vitro*.

In Sec. IV we consider short time scales less than or equal to the period of the oscillation. In this case, the total phase cannot be used to approximate the spike count. We therefore derive the spike count correlation directly, using simple probabilistic reasoning applied to the density of the phase difference. Our analytic results together with Monte Carlo simulations corroborate earlier work showing type II oscillators transfer correlations more readily than type I over short time windows.

II. NOISY OSCILLATORS

Let us begin with a neural oscillator receiving additive noise with equations of motion given by

$$dX = F(X)\,dt + \sigma\xi,$$

where $X \in \mathbb{R}^n$ and ξ is a white noise process. When $\sigma = 0$, we assume the noiseless system has an asymptotically stable periodic solution $X_0(t) = X_0(t+\tau)$ with period τ.

As in the deterministic case, we can reduce this high-dimensional system to a scalar equation for the evolution of the phase θ around the limit cycle. Let $\phi : \mathbb{R}^n \to \mathbb{S}^1$ map a neighborhood of the limit cycle to the phase on a circle. That is, $\theta = \phi(X)$, with $\theta \in [0,1)$. Then θ satisfies

$$\frac{d\theta}{dt} = 1 + \sigma\nabla_X\phi(X)\cdot\xi,$$

where we have normalized the unperturbed period to be 2π. Next we can close the equation by assuming the noise amplitude σ is sufficiently small, so that the system trajectory can be approximated by the noiseless limit cycle X_0:

$$\dot\theta \approx 1 + \sigma Z(\theta)\cdot\xi, \tag{1}$$

where $Z(\theta) = \nabla_X\phi[X_0(\theta)]$ is the adjoint or phase-dependent sensitivity of the trajectory to perturbation along the limit cycle. In the case of a neural oscillator, we assume the noisy perturbations arise as the result of stochastic synaptic input, which influences only the voltage variable. Hence $Z(\theta)$ has only one nonzero component, which is proportional to the phase resetting curve $\Delta(\theta)$.

Thus far, we have used the conventional change of variables to obtain Eq. (1), which therefore must be understood as a stochastic differential equation in the Stratonovich sense. In order to eliminate the correlation between θ and ξ we must use the Itô change of variables, which will introduce an additional drift term:

$$\dot\theta = 1 + \sigma\Delta(\theta)\xi + \frac{\sigma^2}{2}\Delta'(\theta)\Delta(\theta).$$

Here the prime symbol denotes differentiation with respect to θ. For a detailed discussion of phase reduction in noisy oscillators see Ref. [31].

III. CORRELATION TRANSFER OVER LONG TIME SCALES

We now consider the transfer of correlations over time scales much larger than the natural period of the oscillators. Given the level of correlation between the noisy inputs, we wish to know what level of correlation remains between the spike count of two oscillators after some time. For analytic convenience, however, we will use the total phase that has elapsed (modulo 2π) as a proxy for the spike count. Since these quantities differ by at most one, the discrepancy will be negligible for the large spike counts that accrue over long time scales.

Our system will consist of two identical phase oscillators receiving weak, correlated, but not identical, additive white noise. Keeping only terms up to order σ, we have

$$\begin{aligned}\dot\theta_1 &= 1 + \sigma\Delta(\theta_1)\xi_1(t),\\ \dot\theta_2 &= 1 + \sigma\Delta(\theta_2)\xi_2(t).\end{aligned} \tag{2}$$

The noise takes the form

$$\begin{aligned}\xi_1 &= \sqrt{c_{\rm in}}\xi_C + \sqrt{1-c_{\rm in}}\xi_A,\\ \xi_2 &= \sqrt{c_{\rm in}}\xi_C + \sqrt{1-c_{\rm in}}\xi_B,\end{aligned} \tag{3}$$

where ξ_A, ξ_B, and ξ_C are mutually independent, zero-mean white noise processes, and $c_{\rm in} \in [0,1]$ is the correlation between ξ_1 and ξ_2, which we will refer to as the input correlation.

Next let us rewrite Eq. (2) in the form of integral equations:

$$\begin{aligned}\theta_1(t) &= t + \theta_1(0) + \sigma\int_0^t \Delta[\theta_1(s)]\xi_1(s)\,ds,\\ \theta_2(t) &= t + \theta_2(0) + \sigma\int_0^t \Delta[\theta_2(s)]\xi_2(s)\,ds.\end{aligned}$$

Let T be length of the window of time over which we will observe the system. Throughout this discussion we will assume that our system has reached equilibrium, and that time has been reparametrized so that our observation takes place on the interval $t \in [0,T]$. In order to quantify the total phase traversed during this time, we subtract the initial phases by defining $q_i(T) = \theta_i(T) - \theta_i(0)$ for $i = 1,2$. Thus the total phase traversed over a time window of length T is given by

$$q_i(T) = T + \sigma\int_0^T \Delta[\theta_i(s)]\xi_i(s)\,ds,$$

with $q_i(0) = 0$ for $i = 1,2$. Finally, since we assume σ is small, let us simplify the integrands by expanding the phase to lowest order:

$$\theta_i(t) = t + \theta_i(0) + O(\sigma). \tag{4}$$

Then we have $\Delta[\theta_i(s)] = \Delta[s+\theta_i(0)]$, and thus

$$q_i(T) = T + \sigma\int_0^T \Delta[s+\theta_i(0)]\xi_i(s)\,ds. \tag{5}$$

When taking expectations of the quantities in Eq. (5), we must keep in mind that there are four random variables over which averaging must take place. Namely, we must average over the white noise signals $\xi_1(t)$ and $\xi_2(t)$ and the initial conditions $\theta_1(0)$ and $\theta_2(0)$.

Assuming we begin observation after the system has reached equilibrium, we can take one of the initial conditions, say $\theta_1(0)$, to be distributed uniformly on the interval $[0,2\pi]$ because the noise is small. However, at equilibrium the phases obey the steady-state probability distribution $P(\phi)$ derived in Refs. [28,32], which depends only on the phase difference $\phi(t) = \theta_2(t) - \theta_1(t)$. Therefore, the average of Eq. (5) is computed as

$$\begin{aligned}\mathrm{E}[q_i(T)] &= \mathrm{E}\left[T + \sigma\int_0^T \Delta(s+x)\xi_i(s)\,ds\right]\\ &= \frac{1}{2\pi}\int_0^{2\pi}\int_0^{2\pi} P(y-x)\\ &\quad\times\left[T + \sigma\int_0^T \Delta(s+x)\,\langle\xi_i(s)\rangle\,ds\right]dx\,dy\\ &= T + \frac{\sigma}{2\pi}\int_0^{2\pi}\int_0^{2\pi} P(y-x)\\ &\quad\times\int_0^T \Delta[\theta_i(s)]\,\langle\xi_i(s)\rangle\,ds\,dx\,dy = T, \end{aligned}\tag{6}$$

where 2π is the unperturbed period of the oscillators, $P(\phi)$ is the steady-state probability distribution of the phase difference, and x and y represent the initial conditions $\theta_1(0)$ and $\theta_2(0)$, respectively. The last line follows because the white noises have zero mean.

Our goal is to compute the correlation of the total phase traversed by the two oscillators, henceforth referred to as the output correlation c_{out}:

$$c_{\mathrm{out}} := \mathrm{Cor}[q_1,q_2] = \frac{\mathrm{Cov}[q_1,q_2]}{\sqrt{\mathrm{Var}[q_1]\mathrm{Var}[q_2]}}.\tag{7}$$

First, let us derive the covariance as follows:

$$\begin{aligned}\mathrm{Cov}[q_1,q_2](T) &= \mathrm{E}[(q_1(T) - \mathrm{E}[q_1(T)])(q_2(T) - \mathrm{E}[q_2(T)])]\\ &= \mathrm{E}[(q_1(T) - T)(q_2(T) - T)]\\ &= \mathrm{E}\left[\sigma^2\int_0^T \Delta[s+\theta_1(0)]\xi_1(s)\,ds\right.\\ &\quad\left.\times\int_0^T \Delta[s'+\theta_2(0)]\xi_2(s')\,ds'\right] = \sigma^2\frac{1}{2\pi}\\ &\quad\times\int_0^{2\pi}\int_0^{2\pi} P(y-x)\int_0^T\int_0^T \Delta(s+x)\\ &\quad\times\Delta(s'+y)\langle\xi_1(s)\xi_2(s')\rangle ds\,ds'\,dx\,dy\\ &= \sigma^2\frac{c_{\mathrm{in}}}{2\pi}\int_0^{2\pi}\int_0^{2\pi} P(y-x)\int_0^T\int_0^T \Delta(s+x)\\ &\quad\times\Delta(s'+y)\delta(s-s')\,ds\,ds'\,dx\,dy\\ &= \sigma^2\frac{c_{\mathrm{in}}}{2\pi}\int_0^{2\pi}\int_0^{2\pi} P(y-x)\int_0^T \Delta(s+x)\\ &\quad\times\Delta(s+y)\,ds\,dx\,dy.\end{aligned}$$

Similarly, we find the variance to be

$$\begin{aligned}\mathrm{Var}[q_1](T) &= \mathrm{E}[(q_1(T) - \mathrm{E}[q_1(T)])^2]\\ &= \sigma^2\frac{1}{2\pi}\int_0^{2\pi}\int_0^{2\pi} P(y-x)\int_0^T \Delta(s+x)^2\,ds\,dx\,dy.\end{aligned}$$

Note that we therefore have $\mathrm{Var}[q_1] = \mathrm{Var}[q_2]$, and hence the denominator of Eq. (7) can be simplified: $\sqrt{\mathrm{Var}[q_1]\mathrm{Var}[q_2]} = \mathrm{Var}[q_1]$. This gives the output correlation as

$$c_{\mathrm{out}} = c_{\mathrm{in}}\frac{\int_0^{2\pi}\int_0^{2\pi} P(y-x)\int_0^T \Delta(s+x)\Delta(s+y)\,ds\,dx\,dy}{\int_0^{2\pi}\int_0^{2\pi} P(y-x)\int_0^T \Delta(s+x)^2\,ds\,dx\,dy}.\tag{8}$$

Now let $h(x) = \int_0^{2\pi}\Delta(y)\Delta(y+x)\,dy$ be the autocorrelation of the PRC, and let $\phi(t) = \theta_2(t) - \theta_1(t)$ represent the phase difference as before. Then we can rewrite Eq. (8) as

$$c_{\mathrm{out}} = c_{\mathrm{in}}\frac{\int_0^{2\pi} P(\phi)h(\phi)\,d\phi}{\int_0^{2\pi} P(\phi)h(0)\,d\phi}.$$

Note that the right-hand side no longer depends on T after we switched the order of integration and canceled the resulting factors of T in both numerator and denominator. Next we can do away with the denominator entirely, since $h(0)$ does not depend on ϕ, and $P(\phi)$ integrates to one on the interval $[0, 2\pi]$. This leaves simply

$$c_{\mathrm{out}} = c_{\mathrm{in}}\int_0^{2\pi} P(\phi)\frac{h(\phi)}{h(0)}\,d\phi.\tag{9}$$

An explicit expression for the steady-state probability density of the phase difference $P(\phi)$ was derived by Marella and Ermentrout in Ref. [28]. Specifically, we have

$$P(\phi) = \frac{N}{G(\phi)},$$

where $G(x) = 1 - c_{\mathrm{in}}\,[h(x)/h(0)]$, and N is a normalizing constant, $N = 1/\int_0^{2\pi} 1/G(x)\,dx$. Let us further define the PRC to be

$$\Delta(\theta;\alpha) = -\sin(\theta+\alpha) - \sin(\alpha),\tag{10}$$

where α is a parameter that allows us to vary the PRC shape smoothly between type I ($\alpha = \pi/2$) and type II ($\alpha = 0$). See Fig. 1. Using this, the phase distribution over long time scales becomes a function of input correlation and the PRC shape parameter:

$$\begin{aligned}&P(\phi;c_{\mathrm{in}},\alpha)\\ &= \frac{\sqrt{(c_{\mathrm{in}}-1)[\cos(2\alpha)-2][2+(c_{\mathrm{in}}-1)\cos(2\alpha)]}}{2\pi[2-c_{\mathrm{in}}+(c_{\mathrm{in}}-1)\cos(2\alpha)-c_{\mathrm{in}}\cos(\phi)]}.\end{aligned}\tag{11}$$

In the special cases where $\alpha = \pi/2$ and $\alpha = 0$, Eqs. (10) and (11), together with Eq. (8), yield the following:

Type I

$$\begin{aligned}\Delta_{\mathrm{I}}(x) &= 1 - \cos(x)\\ P_{\mathrm{I}}(\phi;c_{\mathrm{in}}) &= \frac{\sqrt{3}}{2\pi}\frac{\sqrt{c_{\mathrm{in}}^2 - 4c_{\mathrm{in}} + 3}}{[3 - 2c_{\mathrm{in}} - c_{\mathrm{in}}\cos(\phi)]}\\ c_{\mathrm{out,I}} &= 1 - \frac{1}{3}\sqrt{3(c_{\mathrm{in}}-3)(c_{\mathrm{in}}-1)}\end{aligned}\tag{12}$$

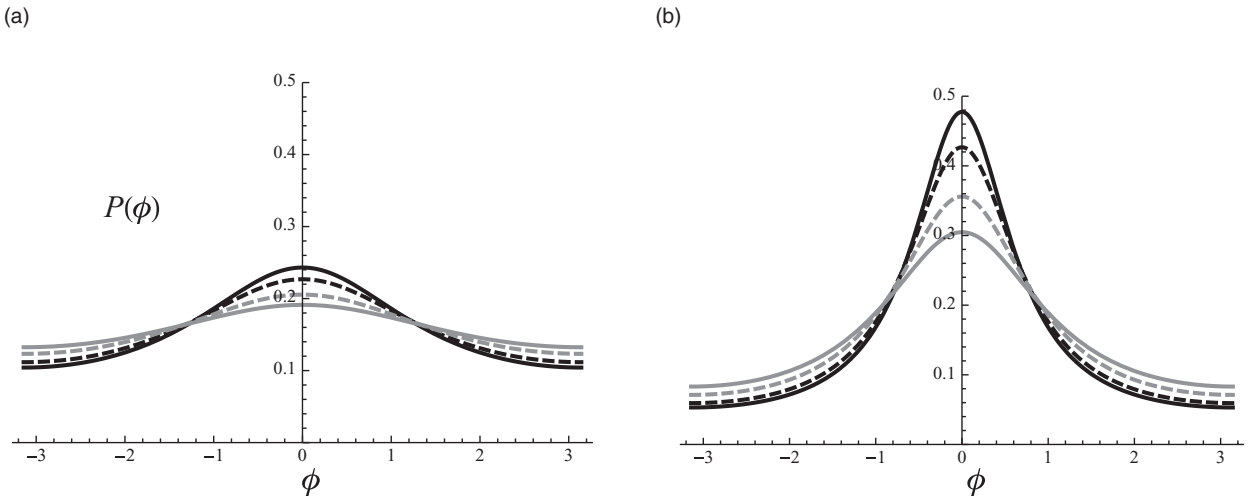

FIG. 2. The steady-state distribution $P(\phi)$ of phase differences ϕ is shown for type I (solid gray) and type II (solid black) as well as for intermediate PRCs (dashed). Note that the unperturbed period of the oscillators is 2π. (a) Input correlation $c_{\text{in}} = 0.4$. (b) Input correlation $c_{\text{in}} = 0.8$.

TypeII

$$\Delta_{\text{II}}(x) = -\sin(x)$$
$$P_{\text{II}}(\phi; c_{\text{in}}) = \frac{1}{2\pi}\frac{\sqrt{1-c_{\text{in}}^2}}{[1-c_{\text{in}}\cos(\phi)]} \tag{13}$$
$$c_{\text{out,II}} = 1 - \sqrt{1-c_{\text{in}}^2}.$$

Figure 2 shows the phase densities for type I and type II PRCs at various input correlations. As in Ref. [30], we see in Fig. 3 that type I oscillators display greater output correlation than type II oscillators for any fixed value of the input correlation c, a surprising finding in light of earlier results that demonstrated the opposite relationship over short windows of observation [19,27–29].

Our intuition for this finding can be honed by performing a further perturbation expansion, now assuming small input correlation. For sufficiently small c_{in}, we can make the approximation

$$\frac{1}{G(x)} = \frac{1}{1 - c_{\text{in}}\frac{h(x)}{h(0)}} \approx 1 + c_{\text{in}}\frac{h(x)}{h(0)}.$$

When we substitute this into Eq. (9) we find

$$c_{\text{out}} = c_{\text{in}}\frac{\tilde{N}}{h(0)}\int_0^{2\pi} h(\phi)\,d\phi + O\left(c_{\text{in}}^2\right), \tag{14}$$

where $\tilde{N} = 1/\int_0^{2\pi}[1 + c_{\text{in}}h(x)/h(0)]dx$ is likewise approximated to lowest order in c_{in}.

The form of Eq. (14) demonstrates that output correlation scales with the integral of the PRC autocorrelation, and for the parametrized PRC in Eq. (10) this integral becomes simply

$$\int_0^{2\pi} h(\phi)\,d\phi = 4\pi^2\sin(\alpha)^2.$$

In particular, $\alpha = 0$ for the type II PRC, and hence $c_{\text{out}} = 0$ to lowest order. Clearly, we have nonzero autocorrelation for nonzero $\alpha \leqslant \frac{\pi}{2}$, and hence PRCs that deviate from pure type II will produce higher output correlation over the long time scales considered here.

Expanding the remaining terms in Eq. (14), we find the approximated output correlation takes the form

$$c_{\text{out}} \approx \frac{2c_{\text{in}}\sin(\alpha)^2}{2 + c_{\text{in}} - (1 + c_{\text{in}})\cos(2\alpha)}. \tag{15}$$

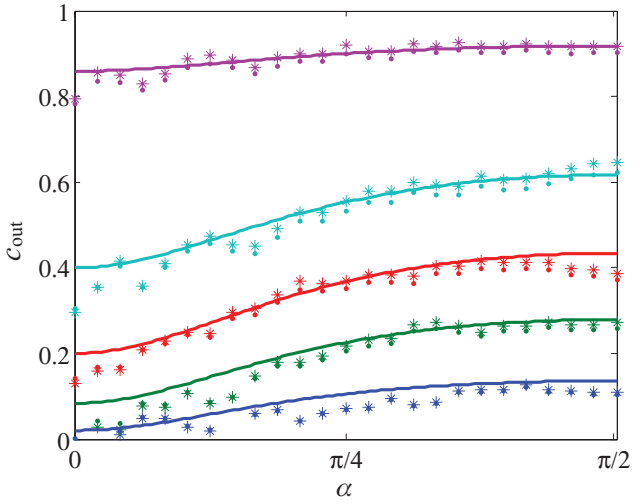

FIG. 3. (Color) Output correlation for large time windows is shown as a function of the PRC shape parameter α. Note that when $\alpha = 0$ the PRC is a pure sinusoid, and therefore the oscillator is type II; when $\alpha = \pi/2$, the oscillator is type I [see Eq. (10)]. Theoretical curves (solid) are a good match for both the simulated total phase correlation (dots) and the simulated spike count correlation (stars). Colors indicate the level of input correlation: 0.2 (blue), 0.4 (green), 0.6 (red), 0.8 (cyan), 0.99 (purple). In all cases, noise amplitude $\sigma = 0.05$, and results are shown for the large time window $T = 50 \times 2\pi$.

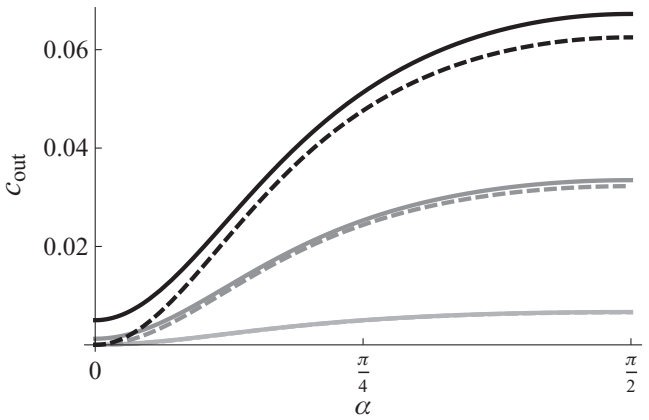

FIG. 4. The perturbation expansion of c_{out} for small input correlation (dashed) agrees well with the full output correlation (solid). Note that, to lowest order in c_{in}, the output correlation goes to zero as the PRC shape parameter α goes to zero, that is, as the PRC shape approaches the pure type II. Colors indicate the level of input correlation: 0.01 (light gray), 0.05 (medium gray), 0.1 (black).

In Fig. 4 we show that this approximation agrees with Eq. (8) for $c_{\text{in}} = 0.01$ and 0.05 but begins to diverge when $c_{\text{in}} = 0.1$. Note that these curves would all lie below the lowest curve plotted in Fig. 3 if shown on the same scale.

We verify the preceding analysis by simulating two phase oscillators perturbed by additive white noise as described in Eqs. (2) and (3). To generate the correlated noise processes of Eq. (3), we first used the MATLAB function randn() to create three independent random vectors of normally distributed values with mean zero and standard deviation one. These vectors correspond to the mutually independent white noise processes ξ_A, ξ_B, and ξ_C in Eq. (3). Then for each correlation value $c_{\text{in}} \in \{0.2,0.4,0.6,0.8,0.99\}$, we created correlated processes ξ_1 and ξ_2 as written in Eq. (3) and repeated here:

$$\xi_1 = \sqrt{c_{\text{in}}}\xi_C + \sqrt{1-c_{\text{in}}}\xi_A,$$
$$\xi_2 = \sqrt{c_{\text{in}}}\xi_C + \sqrt{1-c_{\text{in}}}\xi_B.$$

The oscillators described by Eq. (2) were then integrated using the Euler-Maruyama method [33], specifically for $i = 1,2$:

$$\theta_i(t) = \theta_i(t-1) + dt + \sigma\Delta[\theta_i(t-1)]\xi_i(t-1)\sqrt{dt},$$

with time step $dt = 0.01$ and noise amplitude $\sigma = 0.05$ in all simulations, unless stated otherwise. Note that for convenience, simulations were performed with time rescaled so that $t = T/2\pi$. Therefore the natural period of the oscillators is on the order of one simulation time unit.

Each combination of input correlation c_{in} and PRC shape parameter α was simulated independently for a total duration of 10^5 time units, and the first 10^3 time units were discarded to ensure that the steady-state regime had been reached. We computed the correlation coefficient of both the total phase and the spike count of the resulting oscillator time series over sliding time windows of length T. Figure 3 shows the result for $T = 50$ time units, or 50 times the natural frequency of the oscillators. Both the total phase correlation and the spike count correlation agree closely with each other and with the theoretical curves as a function of the PRC shape parameter α.

IV. SHORT TIME SCALES

Now we will calculate the spike count correlation directly for observation windows T that are shorter than or equal to the natural period, which we assume to be 2π. First, let us consider the probability that a spike occurs in $[0,T]$. We say that oscillator i spikes when its phase θ_i reaches 2π, or in other words $\theta_i(T) \geqslant 2\pi$. Assuming as usual that the noise amplitude σ is small, we expand the phase to lowest order as in Eq. (4), that is, $\theta_i(T) = \theta_i(0) + T + O(\sigma)$. Therefore the probability that oscillator i spikes is simply

$$\mathrm{P}[\theta_i \text{spikes}] = \mathrm{P}[\theta_i + T \geqslant 2\pi],$$
$$\mathrm{P}[\theta_i \text{does not spike}] = \mathrm{P}[\theta_i + T < 2\pi].$$

For two oscillators, there are four possibilities for the joint spike count:

$$\begin{aligned}
&\mathrm{P}[\theta_1 \text{does not spike}, \theta_2 \text{does not spike}] \\
&\quad = \mathrm{P}[\theta_1 + T < 2\pi, \theta_2 + T < 2\pi], \\
&\mathrm{P}[\theta_1 \text{spikes}, \theta_2 \text{does not spike}] \\
&\quad = \mathrm{P}[\theta_1 + T \geqslant 2\pi, \theta_2 + T < 2\pi], \\
&\mathrm{P}[\theta_1 \text{doesnotspike}, \theta_2 \text{spikes}] \\
&\quad = \mathrm{P}[\theta_1 + T < 2\pi, \theta_2 + T \geqslant 2\pi], \\
&\mathrm{P}[\theta_1 \text{spikes}, \theta_2 \text{spikes}] \\
&\quad = \mathrm{P}[\theta_1 + T \geqslant 2\pi, \theta_2 + T \geqslant 2\pi].
\end{aligned}$$

These probabilities can be obtained directly by integrating the density of the phase difference Eq. (11) over the appropriate domain. Note that this gives four discrete joint probabilities for each observation window $T \in [0,2\pi]$. For convenience, let us define the following functions of T:

$$\begin{aligned}
f_{00}(T) &:= \mathrm{P}[\theta_1 \leqslant 2\pi - T, \theta_2 \leqslant 2\pi - T] \\
&= \frac{1}{2\pi}\int_0^{2\pi-T}\int_0^{2\pi-T} P(y-x)\,dx\,dy, \\
f_{01}(T) &:= \mathrm{P}[\theta_1 > 2\pi - T, \theta_2 \leqslant 2\pi - T] \\
&= \frac{1}{2\pi}\int_{2\pi-T}^{2\pi}\int_0^{2\pi-T} P(y-x)\,dx\,dy, \\
f_{10}(T) &:= \mathrm{P}[\theta_1 \leqslant 2\pi - T, \theta_2 > 2\pi - T] \\
&= \frac{1}{2\pi}\int_0^{2\pi-T}\int_{2\pi-T}^{2\pi} P(y-x)\,dx\,dy, \\
f_{11}(T) &:= \mathrm{P}[\theta_1 > 2\pi - T, \theta_2 > 2\pi - T] \\
&= \frac{1}{2\pi}\int_{2\pi-T}^{2\pi}\int_{2\pi-T}^{2\pi} P(y-x)\,dx\,dy.[3pt]
\end{aligned}$$

Figure 5 shows these four functions as T varies between 0 and 2π. Let X be the random variable such that $X = 1$ if θ_1

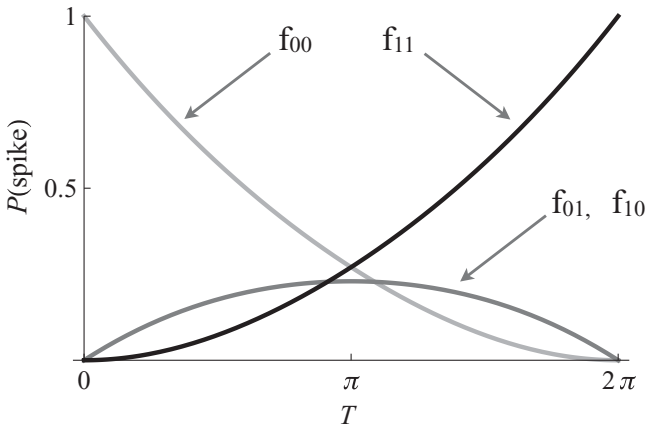

FIG. 5. Joint spiking probability for two oscillators receiving partially correlated noise is shown for observations windows $T \leqslant 2\pi$, where 2π is the natural frequency of the oscillation. The subscripts ij indicate the probability that the corresponding oscillator does (1) or does not (0) spike.

spikes during the observation period T, and $X = 0$ if θ_1 does not spike. Similarly, let Y represent the presence or absence of a spike in oscillator θ_2. Then the covariance is given by $\mathrm{Cov}[X,Y] = \mathrm{E}[XY] - \mathrm{E}[X]\mathrm{E}[Y]$. In terms of the functions defined above we have

$$\begin{aligned}
\mathrm{E}[X] &= 0\cdot(f_{00}+f_{01}) + 1\cdot(f_{10}+f_{11}) \\
&= (f_{10}+f_{11}) = \mathrm{E}[X^2], \\
\mathrm{E}[Y] &= 0\cdot(f_{00}+f_{10}) + 1\cdot(f_{01}+f_{11}) \\
&= (f_{01}+f_{11}) = \mathrm{E}[Y^2], \\
\mathrm{E}[XY] &= 0\cdot 0\cdot f_{00} + 1\cdot 0\cdot f_{10} + 0\cdot 1\cdot f_{01} + 1\cdot 1\cdot f_{11} \\
&= f_{11}.
\end{aligned}$$

A few simplifications are possible. In particular, the sum $f_{10}(T) + f_{11}(T)$ is just the marginal probability that θ_1 spikes within time T. Since θ_1 is uniformly distributed, this probability is simply $\frac{T}{2\pi}$. Furthermore, we also have $f_{10} = f_{01}$ by the symmetry of the density P, and hence $\sqrt{\mathrm{Var}[X]\mathrm{Var}[Y]} = \mathrm{Var}[X]$. Therefore the spike count correlation over short time

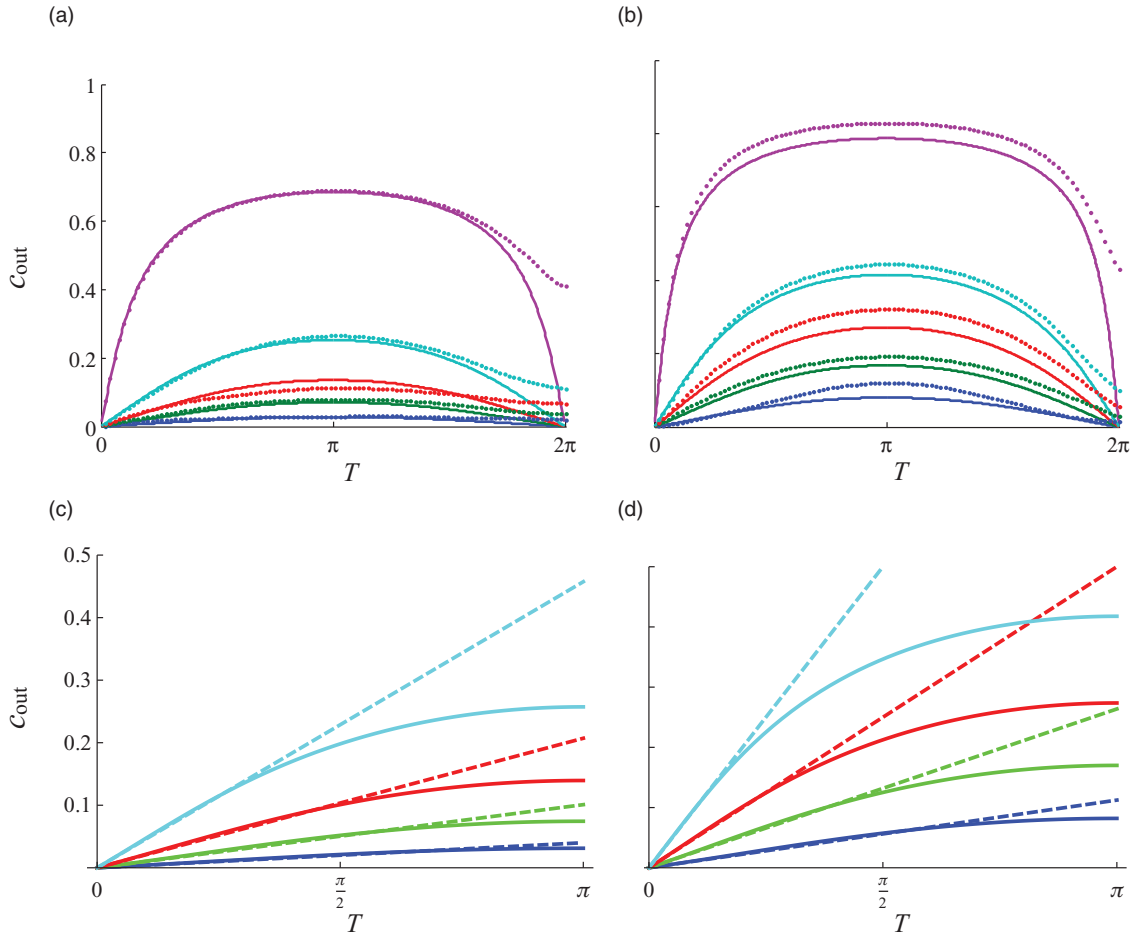

FIG. 6. (Color) (a, b) Theoretical (solid) and simulated (dotted) output correlation curves are shown as a function of the observation window $T \leqslant 2\pi$. (a) Type I oscillators. (b) Type II oscillators. (c, d) The initial slope (dashed) of the spike count correlation (solid) is the linear approximation of Eq. (16) at $T = 0$, given in Eq. (18). (c) Type I oscillators. (d) Type II oscillators. For all plots, noise amplitude $\sigma = 0.05$, and colors indicate the level of input correlation: 0.2 (blue), 0.4 (green), 0.6 (red), 0.8 (cyan), 0.99 (purple).

windows is

$$c_{\text{out}}(T) = \frac{\mathrm{E}[XY] - \mathrm{E}[X]\mathrm{E}[Y]}{\mathrm{Var}[X]} = \frac{f_{11} - (f_{10} + f_{11})^2}{(f_{10} + f_{11})[1 - (f_{10} + f_{11})]} = \frac{f_{11} - \left(\frac{T}{2\pi}\right)^2}{\frac{T}{2\pi}\left(1 - \frac{T}{2\pi}\right)} = \frac{1}{2\pi T - T^2}\left[2\pi \int_{2\pi - T}^{2\pi}\int_{2\pi - T}^{2\pi} P(y - x)\,dx\,dy - T^2\right]. \tag{16}$$

This expression becomes indefinite as $T \to 0$ and $T \to 2\pi$, but a straightforward application of l'Hôpital's rule proves that $c_{\text{out}} = 0$ in these limits. Briefly, let us recall that

$$\frac{d}{dT}\left\{\int_{F(T)}^{2\pi}\int_{F(T)}^{2\pi} P[x,y]\,dx\,dy\right\} = -F'[T]\left\{\int_{F(T)}^{2\pi} P[x,F(T)]\,dx + \int_{F(T)}^{2\pi} P[F(T),y]\,dy\right\}.$$

Thus we have for the numerator of Eq. (16)

$$\lim_{T\to 0,2\pi}\frac{d}{dT}\left[2\pi\int_{2\pi-T}^{2\pi}\int_{2\pi-T}^{2\pi} P(y-x)\,dx\,dy - T^2\right] = \lim_{T\to 0,2\pi}\left[2\pi\int_{2\pi-T}^{2\pi} P(2\pi - T - x)\,dx + 2\pi\int_{2\pi-T}^{2\pi} P(-2\pi + T + y)\,dy - 2T\right].$$

Clearly, as $T \to 0$, the above integrals go to zero, and so the derivative of the numerator is zero. Meanwhile the derivative of the denominator of Eq. (16) evaluates to 2π at $T = 0$. So we have established that $c_{\text{out}} = 0$ at $T = 0$. Similarly, as $T \to 2\pi$ we have for the derivative of the numerator:

$$2\pi\int_0^{2\pi} P(-x)\,dx + 2\pi\int_0^{2\pi} P(y)\,dy - 4\pi.$$

Since $P(\phi)$ is a an even function and, moreover, a probability distribution over phase differences $\phi \in [0, 2\pi]$, the above integrals each evaluate to one. Thus the derivative of the numerator is again zero. Meanwhile the derivative of the denominator of Eq. (16) evaluates to -2π at $T = 2\pi$. Therefore we have established that $c_{\text{out}} = 0$ at $T = 2\pi$ as well.

Figures 6(a) and 6(b) shows how the analytically derived output correlation of Eq. (16) compares with numerical simulations for type I and type II oscillators, respectively, with $\sigma = 0.05$. Correlations were computed for the simulated oscillator time series as described in the previous section; however, now the length of the sliding windows of observation T ranges between 0 and 2π. Note that, although T is short with respect to the natural period of oscillation, the simulated system remains at steady state once the initial transient has been discarded. Therefore the steady-state phase distribution P applies in this setting, and Figs. 6(a) and 6(b) shows good agreement between the analytic and numerical quantities.

We can make a further simplification by considering the linear part of Eq. (16) for T close to zero:

$$c_{\text{out}} = T\left[P(0) - \frac{1}{2\pi}\right] + O(T^2).$$

Thus, the initial slope of the output correlation is proportional to the peak of the stationary distribution of the phase difference, $P(0)$. Substituting $P_I(0)$ and $P_{II}(0)$ from Eqs. (12) and (13), we obtain

$$c_{\text{out,I}} = \frac{T}{\pi}\left[\frac{c_{\text{in}}}{3(1 - c_{\text{in}}) + \sqrt{3(c_{\text{in}} - 1)(c_{\text{in}} - 3)}}\right] = T\frac{c}{6\pi} + O\left(c_{\text{in}}^2\right), \tag{17}$$

$$c_{\text{out,II}} = \frac{T}{2\pi}\left(\frac{1 + c_{\text{in}}}{\sqrt{1 - c_{\text{in}}^2}} - 1\right) = T\frac{c_{\text{in}}}{2\pi} + O\left(c_{\text{in}}^2\right). \tag{18}$$

From here, it is clear that the initial slope of c_{out} is greater for type II than for type I oscillators; in fact, the type II output

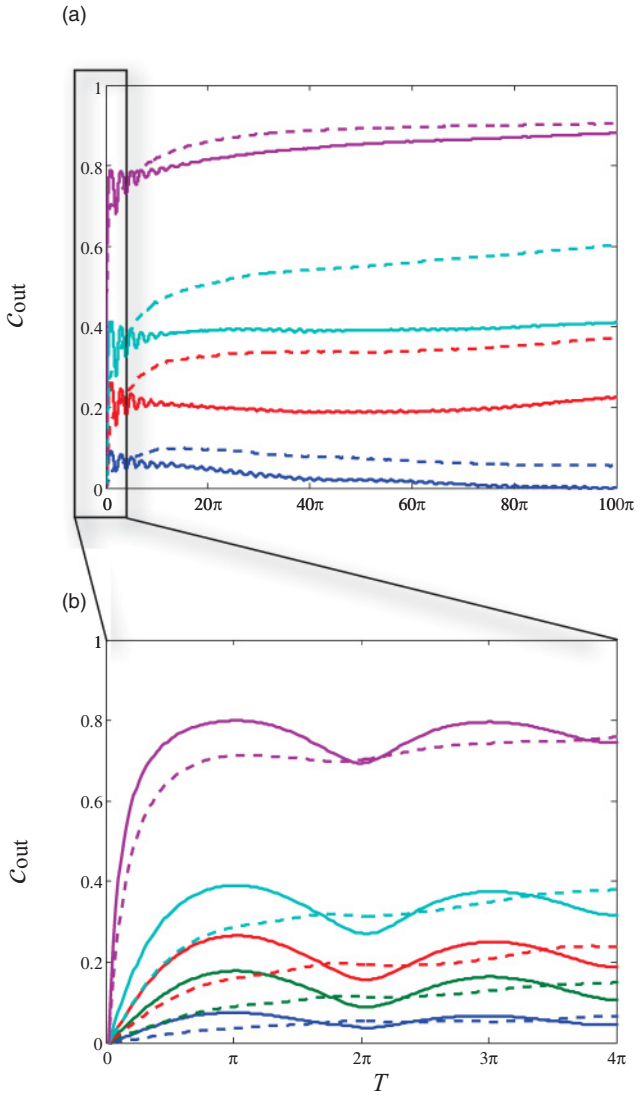

FIG. 7. (Color) Output correlation is shown as a function of intermediate-length observation windows T. Colors indicate the level of input correlation: 0.2 (blue), 0.4 (green), 0.6 (red), 0.8 (cyan), 0.99 (purple). (a) Type II oscillators (solid) exhibit higher output correlations over short time scales than do type I (dashed) over long time scales. (b) This result reverses over short time scales. In all cases, noise amplitude $\sigma = 0.2$.

correlation rises three times faster than the type I, to lowest order in c_{in}. See Figs. 6(c) and 6(d).

V. DISCUSSION

We have demonstrated a novel approach to approximating the spike count correlation of noisy neural oscillators over both long and short time scales. In the case of long windows of observation T much greater than the natural period of oscillation, we used the total elapsed phase (modulo the period) as a proxy for the spike count. The difference between these quantities is at most one and hence is negligible when many spikes are observed over large time windows T. In our perturbation expansion to lowest order in the noise amplitude, σ, the correlation between oscillators depends only on the PRC and the stationary distribution of the phase difference. A further approximation assuming small input correlation c_{in} reveals that output correlation scales with the autocorrelation of the PRC, which is a nonnegative quantity that equals zero precisely when the PRC is a pure sinusoid, i.e., when the oscillator displays type II dynamics. This observation sheds some light on the surprising finding, first reported by Barreiro *et al.* [30], whereby type I oscillators transfer correlations more faithfully than do type II over long time scales, although the reverse holds true for the better understood case of short time scales [19,27–29].

Using straightforward probabilistic reasoning, we computed the spike count correlation directly for short time scales. In the limit of small T and small c_{in}, we obtain an expression for the initial slope of the output correlation, also known as the correlation susceptibility [8]. In Ref. [8] de la Rocha *et al.* use a phenomenological model to explore the complex relationship between susceptibility, firing rate, and threshold nonlinearities. The present analysis illustrates the contribution of bifurcation structure via phase resetting dynamics. In particular, the susceptibility is proportional to the peak of the stationary phase difference distribution, $P(0)$, which in turn depends on the shape of the PRC.

Our analytic expressions in the limit of small noise agree well with spike count correlations computed from simulated oscillators. However, for tractability we included only terms of order one in the perturbation expansion of the phase given in Eq. (4). As a result, the present analysis cannot account for the slow drift of the correlation due to noise, which is visible for values of T near 2π in Fig. 6.

In Fig. 7 the drift is even more apparent. This figure illustrates what happens when we violate all of the assumptions under which the preceding analysis is guaranteed to hold true. In particular, the noise amplitude for the simulations shown in Fig. 7 is 0.2, while for all previous figures, $\sigma = 0.05$. As a result, we see significant drift away from the small noise predictions, even for observation windows as small as $T = 2\pi$. Furthermore, the preceding discussion covers cases where either $T \in [0, 2\pi]$ or $T \gg 2\pi$. The intermediate values of T illustrated in Fig. 7 suggest that type II cells show damped oscillations in output correlation far longer than type I membranes. New analytic methods will be needed to address these and other phenomena at intermediate time scales that may be relevant in biological systems.

[1] P. H. E. Tiesinga, Phys. Rev. E **69**, 031912 (2004).
[2] E. Salinas and T. J. Sejnowski, J. Neurosci. **20**, 6193 (2000).
[3] A. Kuhn, A. Aertsen, and S. Rotter, Neural Comput. **15**, 67 (2003).
[4] T. Tetzlaff, S. Rotter, E. Stark, M. Abeles, A. Aertsen, and M. Diesmann, Neural Comput. **20**, 2133 (2008).
[5] R. C. deCharms and M. M. Merzenich, Nature (London) **381**, 610 (1996).
[6] J. M. Samonds, J. D. Allison, H. A. Brown, and A. B. Bonds, J. Neurosci. **23**, 2416 (2003).
[7] A. Kohn and M. A. Smith, J. Neurosci. **25**, 3661 (2005).
[8] J. de la Rocha, B. Doiron, E. Shea-Brown, K. Josic, and A. Reyes, Nature (London) **448**, 802 (2007).
[9] C. M. Gray, P. Knig, A. K. Engel, and W. Singer, Nature (London) **338**, 334 (1989).
[10] J. Biederlack, M. Castelo-Branco, S. Neuenschwander, D. W. Wheeler, W. Singer, and D. Nikoli, Neuron **52**, 1073 (2006).
[11] M. J. Chacron and J. Bastian, J. Neurophysiol. **99**, 1825 (2008).
[12] K. Josić, E. Shea-Brown, B. Doiron, and J. de la Rocha, Neural Comput. **21**, 2774 (2009).
[13] T. Kreuz, S. Luccioli, and A. Torcini, Phys. Rev. Lett. **97**, 238101 (2006).
[14] E. Zohary, M. N. Shadlen, and W. T. Newsome, Nature (London) **370**, 140 (1994).
[15] K. O. Johnson, J. Neurophysiol. **43**, 1793 (1980).
[16] K. H. Britten, M. N. Shadlen, W. T. Newsome, and J. A. Movshon, J. Neurosci. **12**, 4745 (1992).
[17] W. Bair, E. Zohary, and W. T. Newsome, J. Neurosci. **21**, 1676 (2001).
[18] C. Zhou and K. Jurgen, Chaos **13**, 401 (2003).
[19] R. F. Galán, N. Fourcaud-Trocme, G. B. Ermentrout, and N. N. Urban, J. Neurosci. **26**, 3646 (2006).
[20] D. S. Goldobin and A. Pikovsky, Phys. Rev. E **71**, 045201(R) (2005).
[21] J. N. Teramae and D. Tanaka, Phys. Rev. Lett. **93**, 204103 (2004).
[22] H. Nakao, K. S. Arai, K. Nagai, Y. Tsubo, and Y. Kuramoto, Phys. Rev. E **72**, 026220 (2005).
[23] G. B. Ermentrout, R. F. Galán, and N. N. Urban, Phys. Rev. Lett. **99**, 248103 (2007).
[24] R. F. Galán, G. B. Ermentrout, and N. N. Urban, Phys. Rev. E **76**, 056110 (2007).
[25] K. Yoshimura and K. Arai, Phys. Rev. Lett. **101**, 154101 (2008).
[26] Y. Kuramoto, *Chemical Oscillation, Waves and Turbulence* (Springer, Heidelberg, Germany, 1984).
[27] R. F. Galán, G. B. Ermentrout, and N. N. Urban, J. Neurophysiol. **99**, 277 (2008).
[28] S. Marella and G. B. Ermentrout, Phys. Rev. E **77**, 041918 (2008).
[29] A. Abouzeid and B. Ermentrout, Phys. Rev. E **80**, 011911 (2009).

[30] A. K. Barreiro, E. Shea-Brown, and E. L. Thilo, Phys. Rev. E **81**, 011916 (2010).

[31] J. N. Teramae, H. Nakao, and G. B. Ermentrout, Phys. Rev. Lett. **102**, 194102 (2009).

[32] H. Nakao, K. S. Arai, and Y. Kawamura, Phys. Rev. Lett. **98**, 184101 (2007).

[33] P. Kloeden and E. Platen, *Numerical Solution of Stochastic Differential Equations* (Springer, Heidelberg, Germany, 2010).